rijksuniversiteit groningen

University of Groningen

Bachelor Research Project

Applied Physics

Energetic ions traversing hydrogen gas: Time of Flight and Wien Filter spectrometry

Author:
T.F. Benedictus
S3257444
Daily Supervisor:
S. Rai & K. Bijlsma

Supervisors:
Prof. dr. ir. R. Hoekstra
Prof. dr. S. Hoekstra

August 16, 2020

1 Abstract

The use of EUV light is an important step in the chip manufacturing process. This EUV light is created by laser produced plasma of tin ions. To collect and focus these photons, a collector mirror is placed around the plasma. Hydrogen gas is added to the source chamber to reduce the impact of high energy tin ions on this collector mirror. This thesis provides a look into the Time of Flight and Wien Filter spectrometry methods as possible methods to get insights on the energy and charge state of tin ions after the collision with the hydrogen gas. This is done by using Matlab calculations for the Time of Flight distribution, which is compared to the bunch length of the chopper sweeper system. Simulations of the Wien Filter are done using SIMION and the resulting energy distributions for the different setups are plotted.

Contents

2 Introduction

In 1965 Gordon Moore, co-founder of Intel, made a prediction that computing would increase in power and lower in relative cost at an exponential rate [1]. And nowadays this prediction still holds and is known as Moore's law. Moore's law states that around every two years, the number of transistors on a microchip doubles and the cost is halved [2]. The process of making microchips is called photolithography, which uses a concentrated beam of photons to make a pattern on a substrate wafer. ASML, a company which specializes in lithography technology, is currently the only producer of extreme ultraviolet (EUV) lithography machines [3], shown in figure 1. EUV uses photons with a wavelength of 13.5 nm, which is 14 times lower than the other lithography solution in advanced chip making, deep ultraviolet (DUV) light with a wavelength of 193 nm. Because of the shorter wavelength, EUV lithography can print much smaller features.

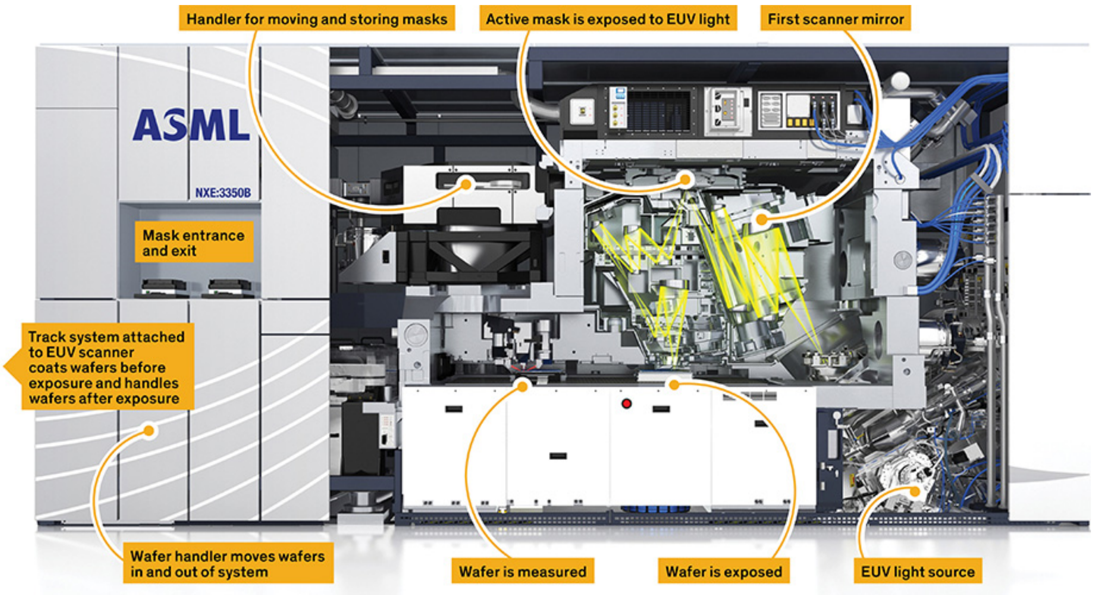

Figure 1: Schematic overview of the EUV lithography machine of ASML. *Image adapted from [4]*

To create the EUV photons, a pulsed laser is shot at a stream of tiny tin droplets. The droplets collect energy, which leads to the forming of laser induced plasma (LPP) that produces highly charged ions which generate the EUV photons. To collect and focus the photons towards the lithography machine, a hemispherical collector mirror is placed around the plasma. However tin ions are ejected as a shower of tin bullets, which in principle can damage the plasma facing equipment. This is a challenge in EUV machines, as the damage to the mirrors leads to a lower yield of EUV photons. To prevent potential damage hydrogen gas is added to the vacuum chamber containing the LPP and collector mirror, which results in an energy loss of the ions due to stopping. However one has to realize that also electron capture occurs, changing the charge state of ions while passing through the stopping gas. This report studies the Time of Flight and Wien Filter methods as a possible way to determine the resulting energy and charge state of energetic tin ions after traversing through hydrogen gas.

3 Theory

3.1 Electron Capture

During the collision of the LPP produced tin ions and the molecular hydrogen gas, charge exchange occurs. For the energy range of the LPP tin ions, the most dominant form of charge exchange is electron capture [5]. During charge exchange, the electrons of the target molecule are transferred to the projectile ion. Resulting in a charge loss of the ion and an ionization of the target molecule. This can be described using the over-barrier-model [5], which is visualized in picture 2 shown below.

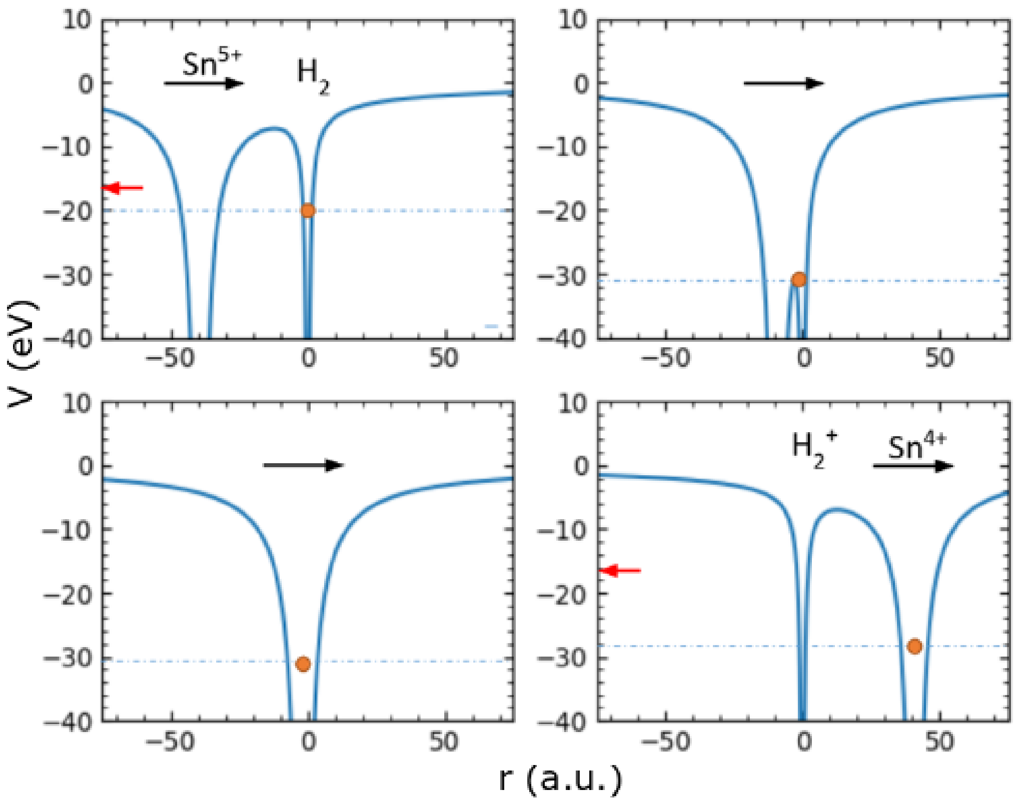

Figure 2: Potential energy diagrams for the over-barrier-model of a Sn^{5+} ion and a hydrogen gas molecule, where r is the distance between the Sn^{5+} ion and the hydrogen gas molecule and V is the potential energy. *Image adapted from [6].*

Here a relatively slow moving projectile ion with a high charge state moves towards a target molecule. When the distance between the target and projectile gets sufficiently small, the Coulomb barrier between the ion and molecule will form a potential well. This allows the electrons to move freely between the ion and the molecule. When the ion passes the molecule, the potential barriers increase again and trap the electron at the ion. Therefore reducing the charge state of the projectile ion and ionizing the target molecule and is described as:

$$A^{q+} + M \rightarrow A^{(q-n)+} + M^{n+} \tag{1}$$

Where A is the projectile ion, M the target molecule, q the initial charge state and n the number of captured electrons by the projectile ion.

3.2 Stopping

When a projectile beam of tin ions collides with a target gas, it will lose some of its energy to the gas. This energy loss is called stopping power and is defined as the energy loss per unit length:

$$\frac{dE}{dx} = -NS = -N(S_e + S_n) \tag{2}$$

Where S is the stopping cross section and N is the number of target particles per $[m^3]$. The stopping power consist of two classes, the electronic and nuclear stopping power. The electronic stopping power is due to the interaction between the ion and the electrons of the target. Nuclear stopping power is due to the energy loss from the screened-off potentials of the nuclei of the projectile and target particle [7]. In general, electronic stopping power is stronger than nuclear stopping power. However this only holds for higher orders of the kinetic energy, as shown in figure 3.

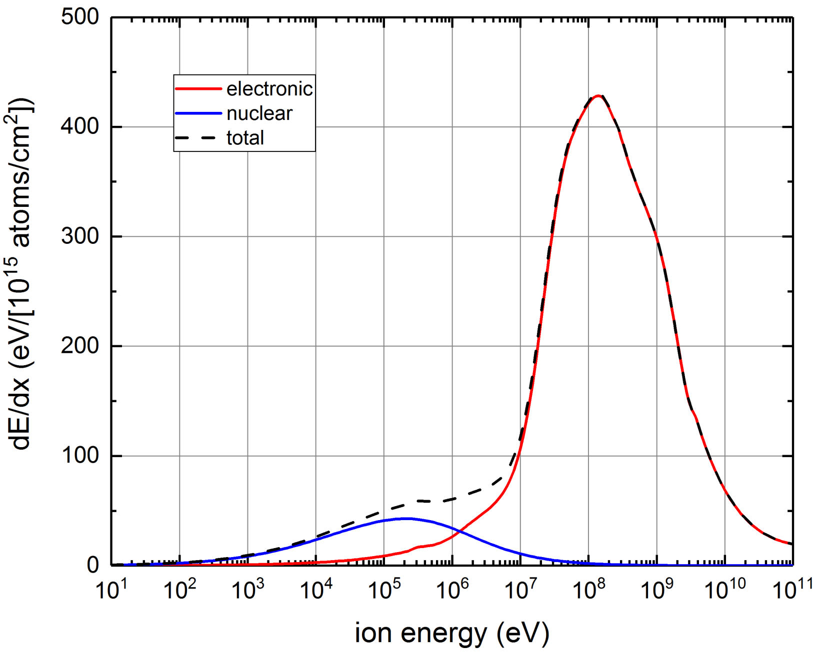

Figure 3: The nuclear (blue), electronic (red) and total stopping power (- -) for tin projectiles in hydrogen gas. *Data extracted from SRIM.*

Tin ions ejected from an LPP-source generally are below 20 keV and for this experiment a kinetic energy of 1 keV is used for the tin particles. For a lower energy range as shown in figure 4, it can be shown that nuclear stopping power is the dominant factor.

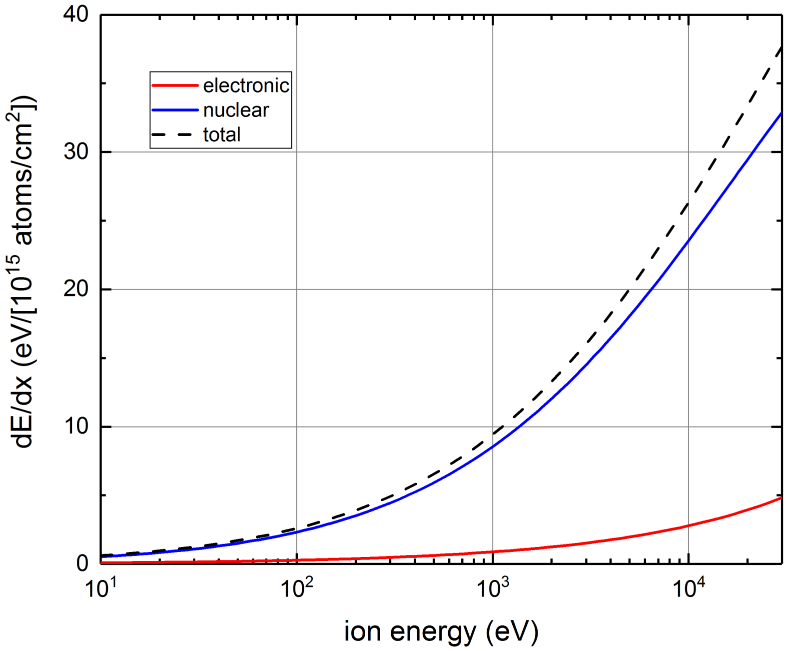

Figure 4: The nuclear (blue), electronic (red) and total stopping power for tin projectiles in hydrogen gas for energy range from 0.01 to 30 keV. *Data extracted from SRIM.*

3.3 Time of Flight

To identify the energy loss of the tin ion beam after the collision with the hydrogen gas, several spectrometric methods can be used. One of them is Time of Flight. As the name suggest, Time of Flight looks at the time it takes a particle to travel from point a to b. The travel time is determined by

$$t = \frac{d}{v} = \frac{d}{\sqrt{\frac{2E}{m}}} \tag{3}$$

where d is the travel distance, E is the energy of the particle and m is the mass of the particle. This equation results in different travel times for particles with different kinetic energies. In order to conduct experiments, the continuous beam is pulsed by a chopper system as shown in figure 5 [6]. This creates ion bunches of length τ_b shown in figure 6 and is given by

$$\tau_b = \frac{5.11 * 10^{-5}}{v_0} \frac{V_{ECR}}{V_{ch}} \tag{4}$$

where v_0 is the initial velocity of the ion beam and V_{ECR}/V_{ch} is the ratio between the source acceleration voltage and the chopper voltage.

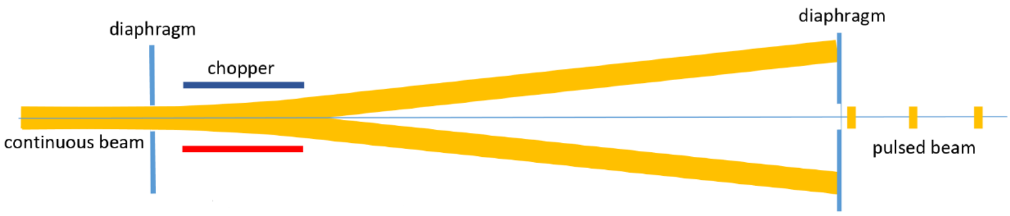

Figure 5: Schematic overview of the conversion of a continuous beam into a chopped beam. *Image adapted from [6]*

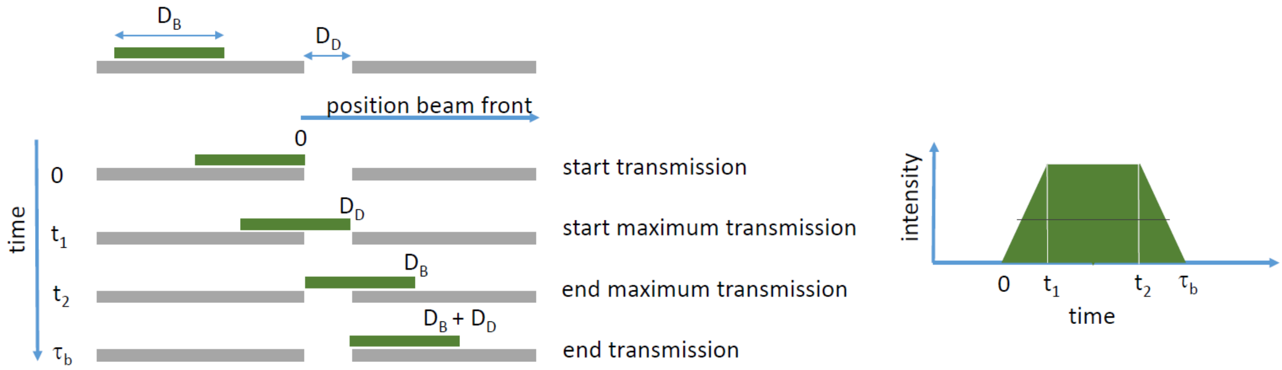

Figure 6: Schematic representation of the creation of pulse length τ_b for the chopper sweeper system.

The full width half maximum of the pulse length τ_b is given by

$$FWHM = \frac{D_B}{D_B + D_D}\tau_b \tag{5}$$

where D_B is the beam diameter and D_D is the aperture diameter, as is shown in figure 6. The values of D_B and D_D are given by $D_B = 3.6\ mm$ and $D_D = 1\ mm$ [6]. This gives a FWHM of the pulse length of $FWHM = 19.6\ ns$.

3.4 Wien Filter

Another possible way to determine the energy of the outgoing tin ion beam is with the use of a Wien Filter. A Wien Filter uses crossed magnetic and electric fields to separate charged particles based on difference in velocity. The charged particle species of interest with a velocity v_0 travels in a straight line through the orthogonal electric and magnetic fields if the Wien condition, $v_0 = E/B$ with $\vec{v}\perp\vec{E}\perp\vec{B}$, is satisfied [8]. All other species are suppressed as shown in Figure 7.

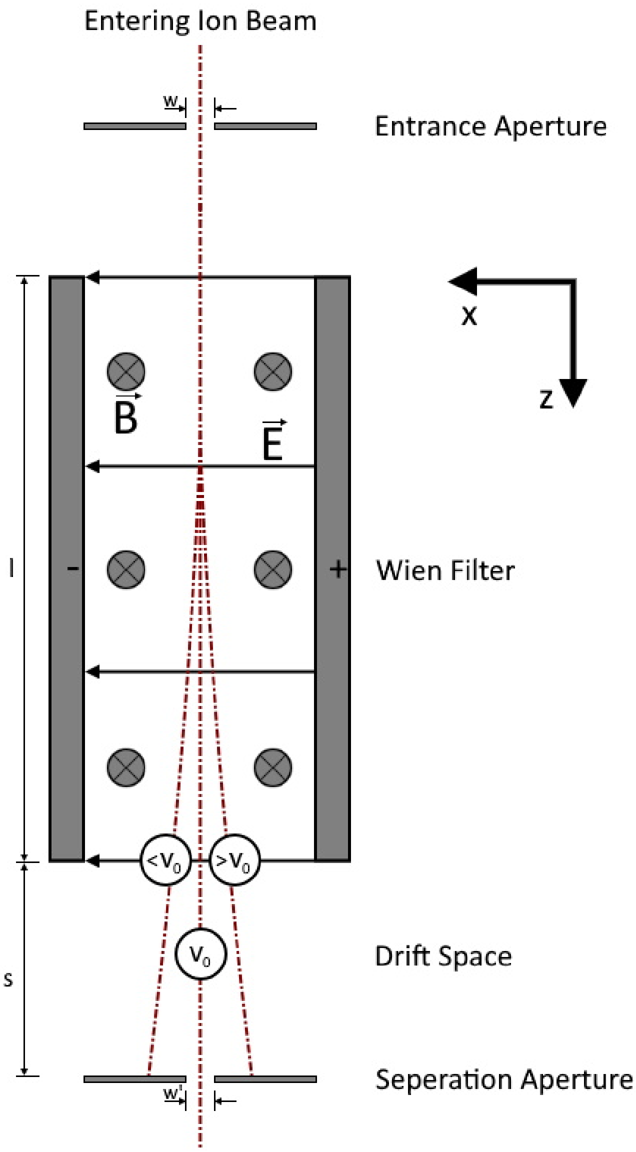

Figure 7: Functional principle of the Wien Filter. *Image adapted from [8].*

For an electric field $\vec{E} = E\vec{e_x}$ and a magnetic field $\vec{B} = B\vec{e_y}$, the equation of motion for a particle with charge q are given by

$$m\ddot{x} = qe(E - B\dot{z}) \tag{6}$$

$$m\ddot{y} = 0 \tag{7}$$

$$m\ddot{z} = qeB\dot{x} \tag{8}$$

with the unit charge $e = 1.6 \times 10^{-19}$ C. The x- and z-coordinate describe the transverse (x) and longitudinal (z) position of the particle relative to the initial beam line.

As the charged particles travel perpendicular to both the electric and magnetic field at $x = z = 0$. The solution of x(t) and z(t) for initial conditions $v_{x,0} = 0, v_{y,0} = 0$ and $v_{z,0} = v_0$ is given by

$$x(t) = \frac{m}{qeB}\left(v_0 - \frac{E}{B}\right)\left(cos\left(\frac{qeB}{m}t\right) - 1\right) \tag{9}$$

$$z(t) = \frac{m}{qeB}\left(v_0 - \frac{E}{B}\right) sin\left(\frac{qeB}{m}t\right) + \frac{E}{B}t \tag{10}$$

For the Wien condition, $v_0 = E/B$, the motion of the charged particle becomes linear and steady along the z-direction.

$$z(t) = \frac{E}{B}t = v_0 t \tag{11}$$

For charged particles travelling through the Wien filter of length l, the transverse deviation is small compared to l ($v_0 \approx E/B$). Therefore the first term of equation (10) can be omitted, which results in a time-dependence of z(t) as described in equation (11). Eliminating the time dependence of equation (9) using equation (11), the trajectory x(z) inside the filter is approximated by

$$x(z) = \frac{m}{qeB}\left(v_0 - \frac{E}{B}\right)\left(cos\left(\left(\frac{qeB^2 z}{mE}\right) - 1\right)\right) \tag{12}$$

To improve the resolution of the Wien filter, a drift space is added. It has a length s and is approximately field free. This amplifies the deviation of the particle in the transverse (x) direction. Using equation (12), the approximate expression for the total transverse deviation of the Wien filter with drift space is given by:

$$x(l+s) = \frac{m}{qeB}\left(v_0 - \frac{E}{B}\right)\left(cos\left(\frac{qeB^2 l}{mE}\right) - 1\right) + s\left(1 - \frac{B}{E}v_0\right) sin\left(\frac{qeB^2 l}{mE}\right) \tag{13}$$

4 Simulation Setup

4.1 Time of Flight

To see if the Time of Flight method is a viable solution to determine the energy of the tin ions that traversed a gas cell in which they lost a fraction of their energy, a simulation is done using Matlab. Therefore the travel time of 1 keV Sn^{5+} is compared to a set of Sn^{5+} particles with a normal distribution for the energy and starting position. For energy, the normal distribution has $mean = 1\ keV$ and $FWHM = 5 \cdot q = 25\ eV$ [9]. The normal distribution in the starting position has $mean = 0mm$ and $FWHM = 3.5\ mm$. The FWHM of the time delay is then compared to the bunch length created by the chopper sweeper system.

4.2 Wien Filter

The simulated model of the Wien Filter is based on the DREEBIT Wien Filter. It consists of two parallel electrodes with a gap in between. Perpendicular to the electrodes, a magnetic yoke can be placed. A weak magnetic yoke, $B = 0.14\ T$, which is used for low mass applications. And a

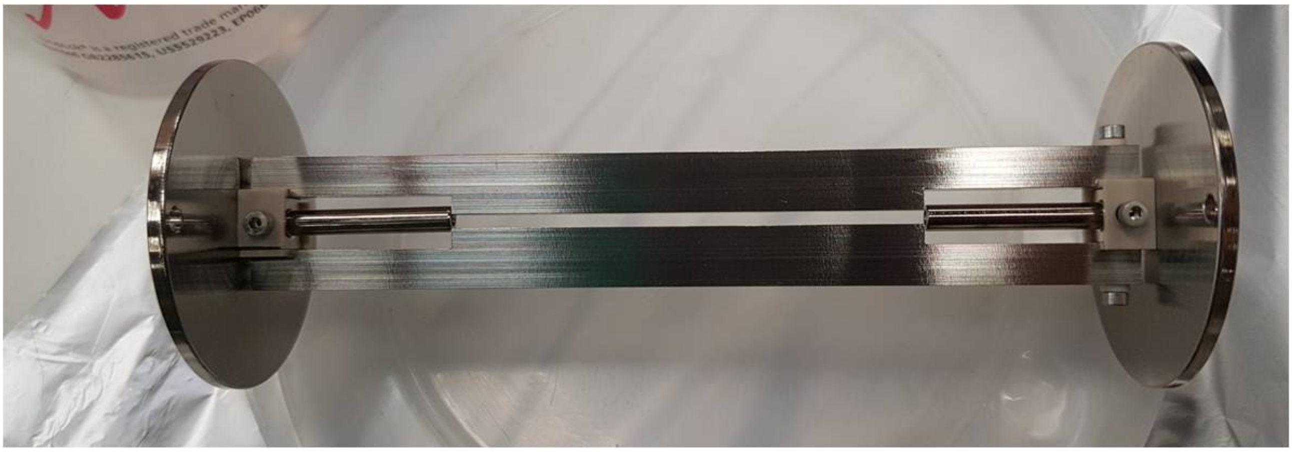

Figure 8: The electrodes, tubes and aperture of the disassembled DREEBIT Wien Filter.

strong magnetic yoke, $B = 0.52\ T$, which is used for broad mass and charge range applications. The DREEBIT Wien Filter comes with 3 different size apertures, 0.5 mm, 1.0 mm and 1.5 mm. The smaller apertures result in a higher resolution, but a lower transmission.

Two grounded tubes are located just after the first aperture and just before the second aperture, see figure 8 and the schematic drawing shown in figure 9. These reduce the effect of the stray magnetic and electric field on the charged particle.

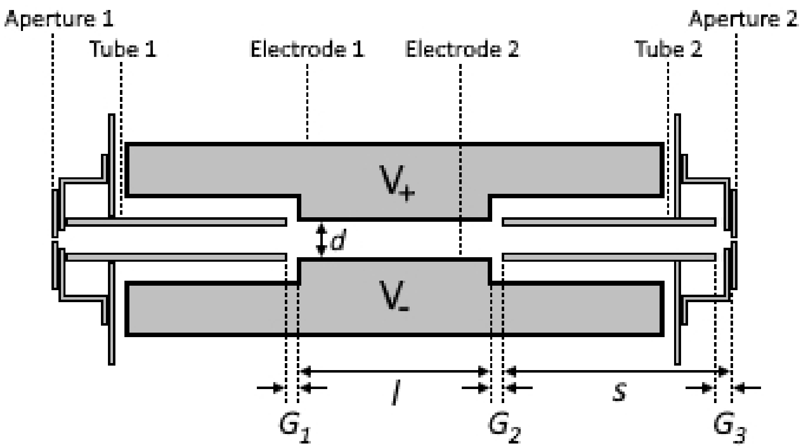

Figure 9: Schematic drawing of the electrodes, tubes and aperture of the DREEBIT Wien Filter.

To model this Wien Filter, more specific dimensions are needed besides the total length of 150 mm. The gap d between the electrodes is $d = 2\ mm$, length l of the electrodes $l = 70.0\ mm$ and the drift space $s = 39.0\ mm$. The gaps between the electrodes and tubes are $G_1 = G_2 = 0.5\ mm$ and the gap between the right tube and aperture is $G_3 = 10\ mm$.

4.3 SIMION

In this work, SIMION is used to model the DREEBIT Wien Filter and simulate the trajectories of energetic tin ions in it. SIMION is a field and particle trajectory simulator [10]. Here a brief description of working in SIMION will be given.

First a potential array has to be defined. A Potential Array is a grid of points in which the points can be given a certain potential, magnetic or electrostatic, or it can be set as an (non-)electrode point [10]. The potential array is refined, which calculates the electric and magnetic fields using the Laplace equation, and can be used in a workbench. A workbench links one or more potential arrays with ion definitions and data recording.

Several SIMION models of the WIEN filter are created. A typical model with an exit and with different apertures and alignment of electrodes and tubes. Figure 10 shows the model for the $0.5mm$ aperture with parallel tubes and electrodes.

Figure 10: The basic Wien Filter SIMION model with apertures of 0.5 mm and parallel tubes and electrodes.

For the electric potential array of the Wien Filter, the electrodes, are set as fast adjustable electrodes with a certain potential with $V_{-} = -V_{+}$. Resulting in a potential difference between the electrodes of $\Delta V = 2V_{+}$. Fast adjustable electrodes can be changed directly in the workbench. The tubes and apertures are set as electrodes with a potential of zero. This means that the parts are grounded and particles will collide with the electrodes. For the magnetic field, a second potential array has to be added. It is set as a magnetic potential array and is given a width equal to the length of the electrodes l. In the workbench, this potential array is then placed on top of the electrodes. Using a user program, a magnetic field with strength B and a negative y-direction is assigned to the magnetic potential array.

The optimal potential difference, $\Delta V_{optimal}$ for ions with certain energy is first calculated for a given magnetic field B to find the neighbourhood. As the calculated potential differs from the optimal potential for the simulation, the value is manually tuned to the best value. However the potential on the electrodes have a minimal step size of 0.1 V defined by the power supply [8]. Therefore $\Delta V_{optimal}$ is chosen to be the closest value in according to the step size of the power supply.

5 Results

The goal is to verify if Time of Flight and Wien Filter spectrometry methods could be used to give more information about the reaction products between the collision of energetic tin ions and molecular hydrogen gas. For the Time of Flight this is done by looking at the distribution of the travel time for a given distribution of energetic tin particles. For the Wien Filter, the measured energy distribution is compared to a given incoming energy distribution. All calculations and simulations were done using Sn-120 ions with an energy distribution with $mean = 1\ keV$ and $FWHM = 25\ eV$.

5.1 Time of Flight

The Time of Flight is independent on the charge state of the Sn-120. Therefore only depends on the mass, energy and starting position. The total distribution of Sn-120 with mass $m = 120\ u$, the energy distribution as stated in the section above and a distribution in the starting position with $mean = 0\ mm$ and $FWHM = 3.5 \cdot 10^{-3}\ m$, is shown in figure 11 below.

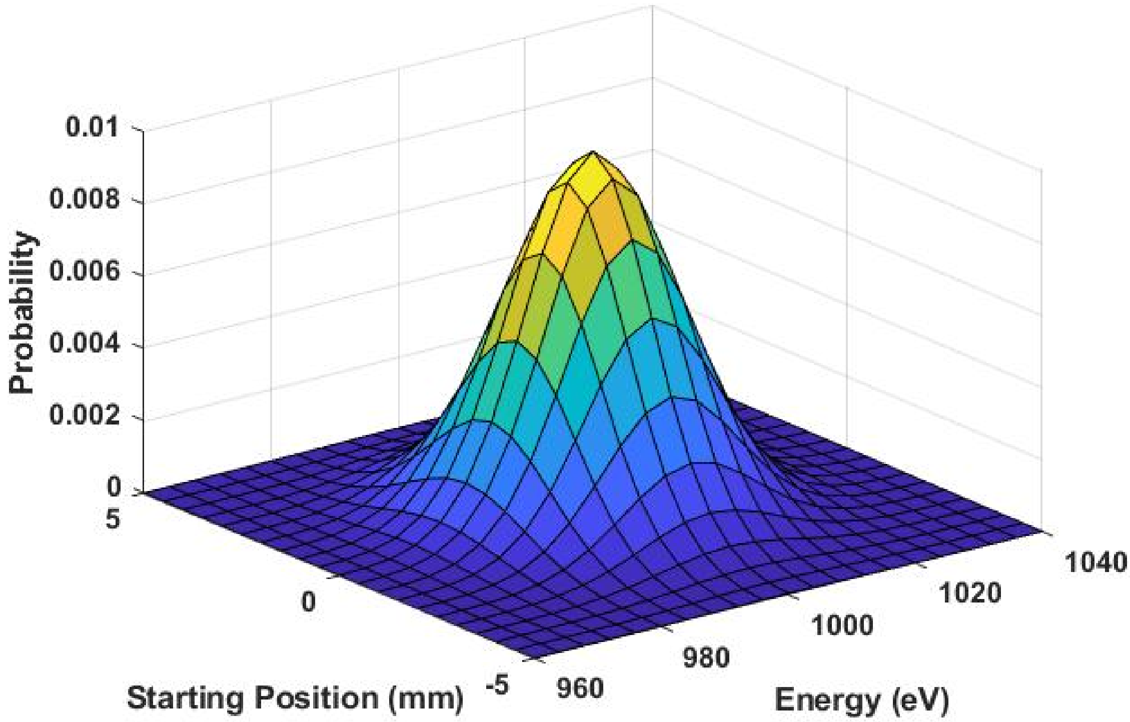

Figure 11: Probability distribution for the starting position, $mean = 0$ and $FWHM = 3.5 \cdot 10^{-3}\ m$. And the energy distribution, $mean = 1\ keV$ and $FWHM = 25\ eV$.

It has a peak for the probability of particles being near 1 keV and 0 mm. With this distribution, calculations were done for a travel distance of 20 cm. The Time of Flight of the particles is then compared to the Time of Flight of a reference Sn-120 particle with a starting position of 0 mm and an energy of 1 keV. This results in a distribution in the time delay, which is shown in figure 12.

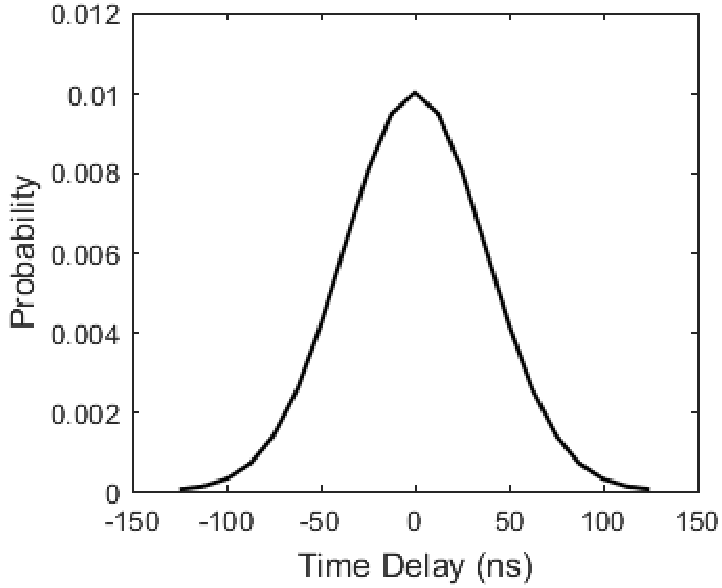

Figure 12: Time delay probability distribution for Sn-120 with an energy and starting position distribution compared to 1 keV, 0 mm Sn-120.

It shows a normal distribution with $FWHM = 74.8\ ns$ and $mean = 0\ ns$. This is according to the expectations, as for the given distributions more particles are closer to the reference particle. The FWHM of the bunch length, 19.6 ns, is significantly lower than the FWHM of the time delay, 74.8 ns. Therefore the influence of the bunch length on the Time of Flight calculations is negligible.

5.2 Wien Filter

5.2.1 Magnetic yokes

The DREEBIT Wien Filter, comes with two different magnetic yokes of 140 mT and 520 mT. For heavy particles such as Sn-120, the manufacturer suggest to use the stronger magnetic yoke. This is to create a larger deviation for the different charge states of the particles. This would result in better distinguishable peaks for each different charge state. Along with the energy, the charge state of the energetic tin ions after collision with molecular hydrogen gas is also of interest. Therefore the effects of the magnetic yokes on the different charge states of Sn-120 ranging from $q = 0$–5 are compared.

For the strong magnetic yoke, $B = 520\ mT$ and $\Delta V = 42\ V$, the optimised voltage difference for a 1 keV particle with $q = 5$, the distribution of the different charge states is shown in figure 13. A neutral particle with $q = 0$ does not experience any electric and magnetic field. Therefore all particles with charge state $q = 0$, independent on the energy, reach the measurement point after the last aperture. Which will result in a larger energy distribution.

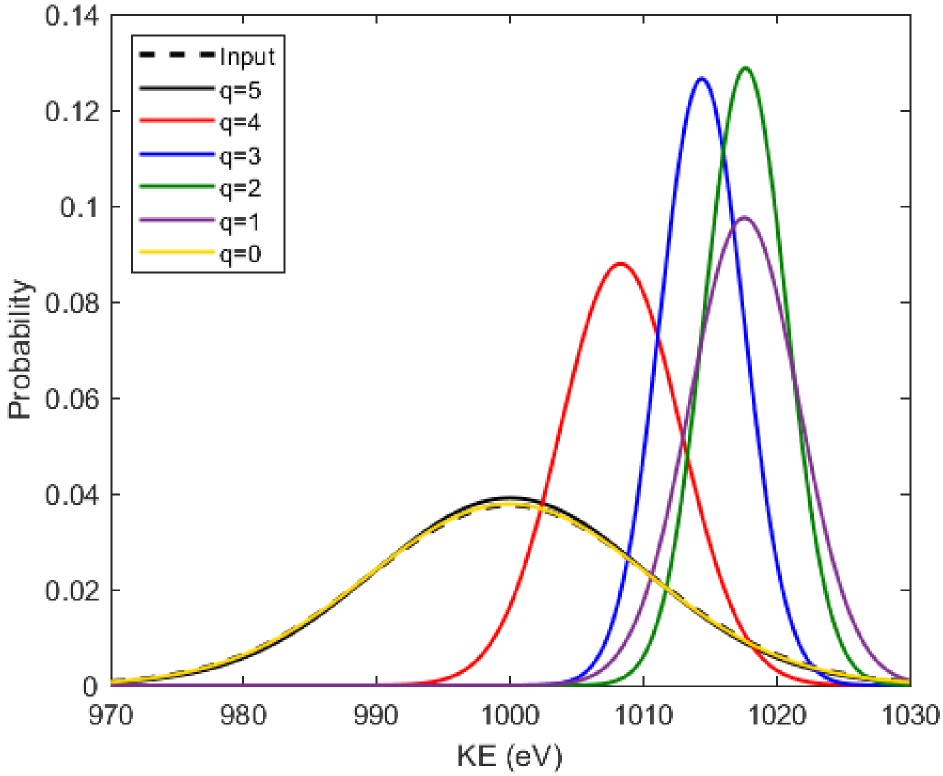

Figure 13: Scaled (to area) energy probability distribution for different charge states of Sn-120 ions passing through the Wien Filter using the strong magnetic yoke, $B = 520\ mT$. All ions have the same initial energy distribution (input).

As expected, the energy distribution for $q = 0$ is almost identical to the energy distribution of the input beam. This means that the energy distribution of the neutral particles are not affected on passing through the Wien filter which is expected as neutrals do not experience any fields. For $q = 5$, it shows a higher peak and slightly lower wings then the input beam. The charge states $q = 1$–4 show a shift of the peak to the right compared to the input beam. Thus only higher energy particles with those charge states reach the measurement point, i.e. the Wien Filter acts as a high-pass filter for lower charge states. The mean and standard deviation σ of the different charge states are given in table 1 below.

q	Mean (eV)	σ (eV)
Input	1000.0	10.62
0	999.93	10.56
1	1017.6	4.092
2	1017.7	3.099
3	1014.4	3.153
4	1008.3	4.538
5	1000.0	10.22

Table 1: Mean and standard deviation of the different charge states of Sn-120 using the strong magnetic yoke, $B = 520\ mT$, in the Wien Filter.

Table 1 and figure 13 only show the distributions, but do not take into account the amount of counts that each charge state has. Therefore for each charge state with an input beam with 1000 counts, the measured counts are plotted against the energy. This is shown in figure 14.

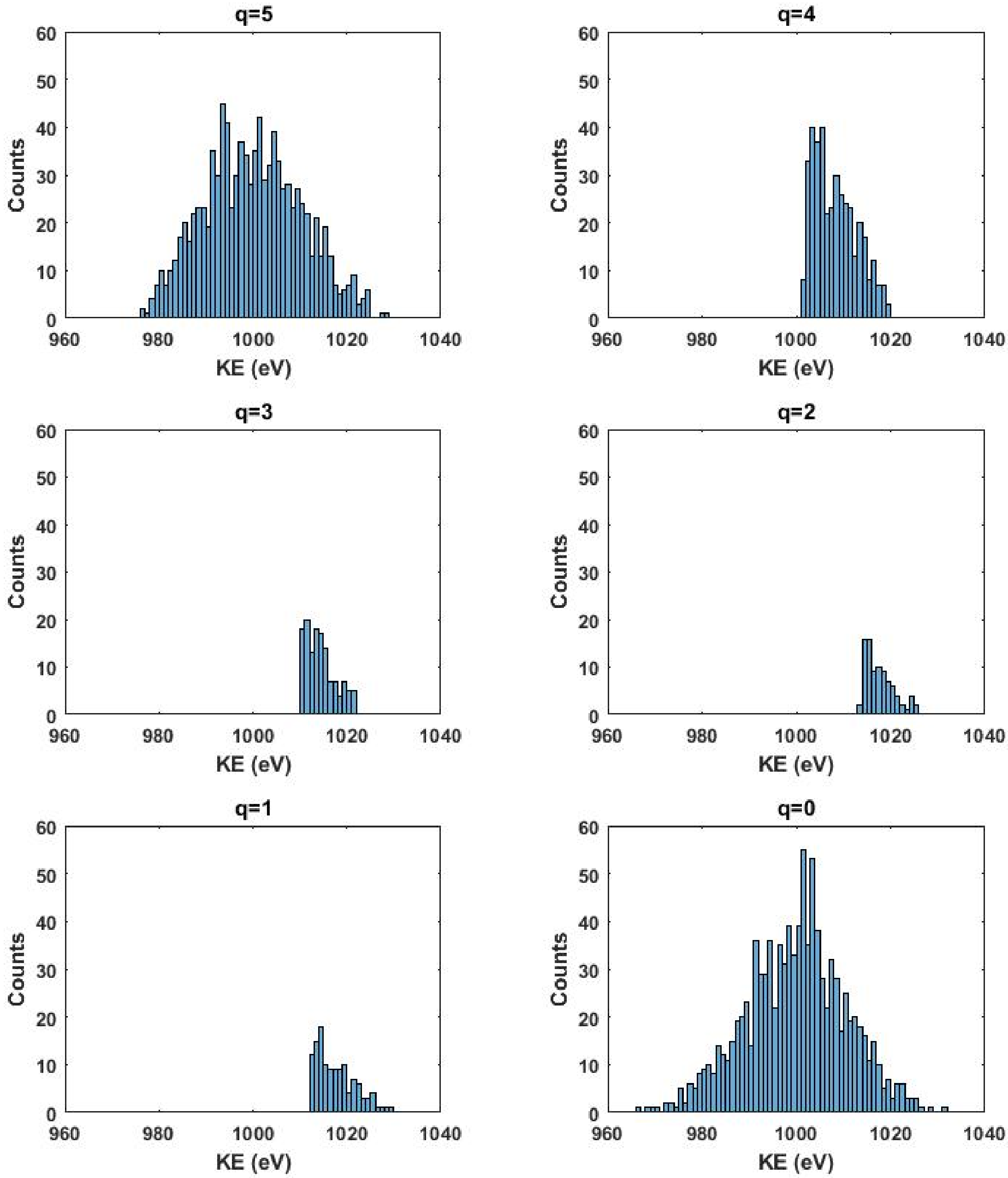

Figure 14: Amount of measured particles with certain energy for $B = 520\ mT$ and $\Delta V = 42\ V$ for charge states $q = 0$–5. With an input beam of 1000 particles.

As expected $q = 0$ and $q = 5$ have the highest total counts. With the total counts decreasing for $q = 4$ to $q = 1$. The optimised $\Delta V = 42\ V$ for $q = 5$ shows an overlap in the energy distributions for the different charge states. This is due to the distribution in the input energy beam, which leads to lower charged particles with higher energy that can still travel to the measurement point. Therefore the different charge states can not be fully distinguished from each other using the strong magnetic yoke. However, the high-pass nature of the filter can help to get information on the fraction of ions that loose an appreciable part (10–20 eV) of their kinetic energy.

For the weak magnetic yoke with $B = 140\ mT$ and the optimised voltage difference for a 1 keV particle with $q = 5$, $\Delta V = 11.14\ V$, the distribution of the different charge states is shown in figure 15.

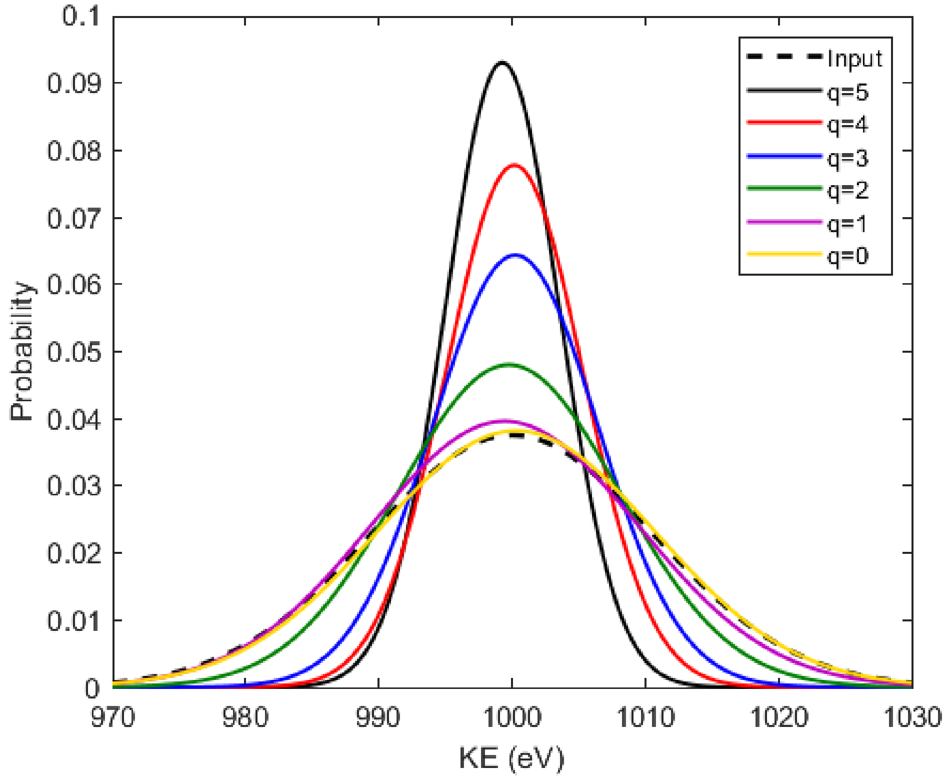

Figure 15: Energy probability distribution for different charge states of Sn-120 using the weak magnetic yoke, $B = 140\ mT$, in the Wien Filter.

As expected the weaker magnetic yoke does not have a big effect on the peak of the different charge state distributions. It does however show that the energy range of the lower charge states is significantly larger than the higher charge states. Looking at equation 13, it shows that for smaller q the cosine term is closer to 1 and the sine term is closer to 0. This implies that for the same energy distribution of the incoming particles, the distribution in the x-direction is lower for smaller q. This leads to the more narrow distribution of energy measured for higher charge states q. The mean and standard deviation

σ of the charge states shown in figure 15 is given in table 2 below.

q	Mean (eV)	σ (eV)
Input	1000.0	10.62
0	999.93	10.56
1	1017.6	4.092
2	1017.7	3.099
3	1014.4	3.153
4	1008.3	4.538
5	1000.0	10.22

Table 2: Mean and standard deviation of the different charge states of Sn-120 using the weak magnetic yoke, $B = 140\ mT$, in the Wien Filter.

Just as for the stronger magnetic yoke, an input beam of a 1000 particles for each charge state is simulated. The count distribution of the measured particles are shown in figure 16.

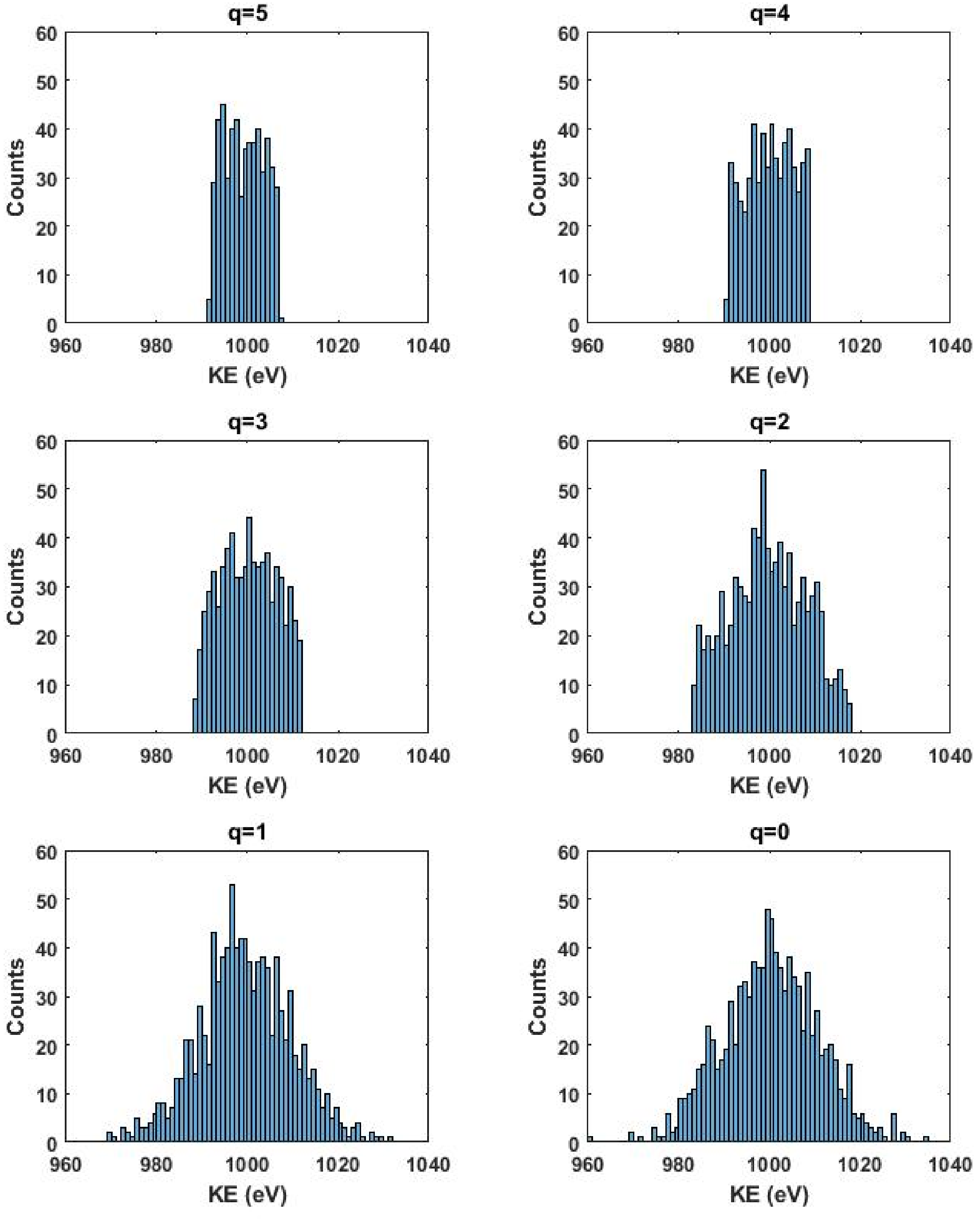

Figure 16: Amount of measured particles with certain energy for $B = 140\ mT$ and $\Delta V = 11.2\ V$ for charge states $q = 0$–5. With an input beam of 1000 particles.

Thus for the weaker magnetic yoke, all charge states have energy distributions that peak around 1 keV. Therefore the Wien Filter could be used to determine the energy of the energetic tin ions after traversing the stopping gas.

5.2.2 Apertures

To determine the influence of the size of the different apertures, a simulation is done for each aperture with different voltages on the electrodes. The simulation uses the weak magnetic yoke, $B = 140\ mT$, and a 3000 Sn-120 beam with an arithmetic sequence ranging the charge state from 3 to 5. Therefore there are 1000 Sn-120 ions per charge state and all charge states have the same energy distribution as stated earlier. The highest peak of particles is obtained for a voltage difference $\Delta V = 11.14\ V$. As the voltage on the electrodes have a minimal step size of 0.1 V defined by the power supply, three different ΔV were taken around this point, $\Delta V = 11.0\ V$, $\Delta V = 11.2\ V$ and $\Delta V = 11.4\ V$.

For the aperture of 1.5 mm the results are shown in figure 17.

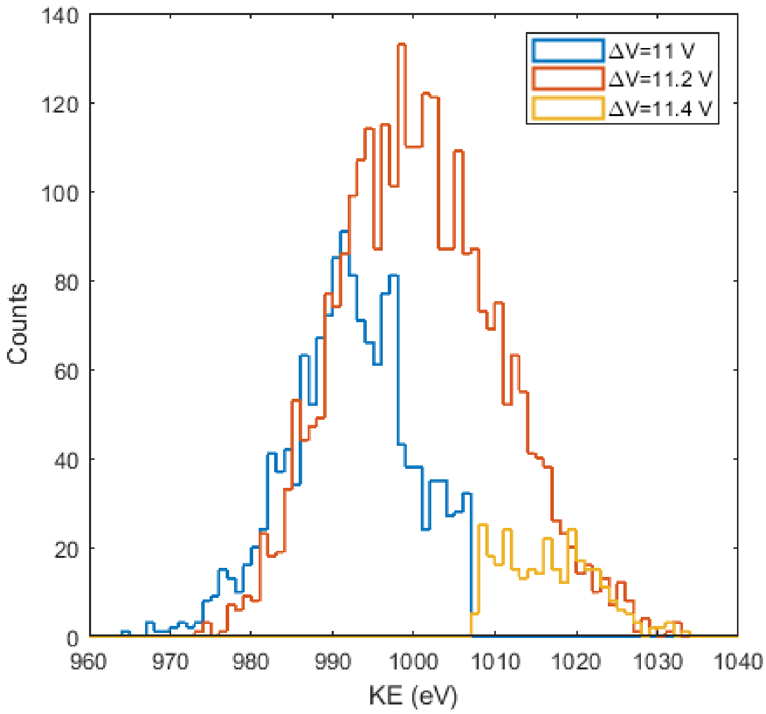

Figure 17: Energy distribution of Sn-120 ions with charge states ranging from 3 to 5 using an aperture of 1.5 mm for different voltages ΔV between the electrodes.

As $\Delta V = 11.2\ V$ is the closest to $\Delta V = 11.14\ V$, it is expected to have the highest total number of counts. Looking at figure 17 it indeed shows the highest counts and the most uniform distribution. However the distribution does have a wide spread.

The same process is repeated for apertures 1.0 mm and 0.5 mm. These are shown in figures 18 and 19 respectively.

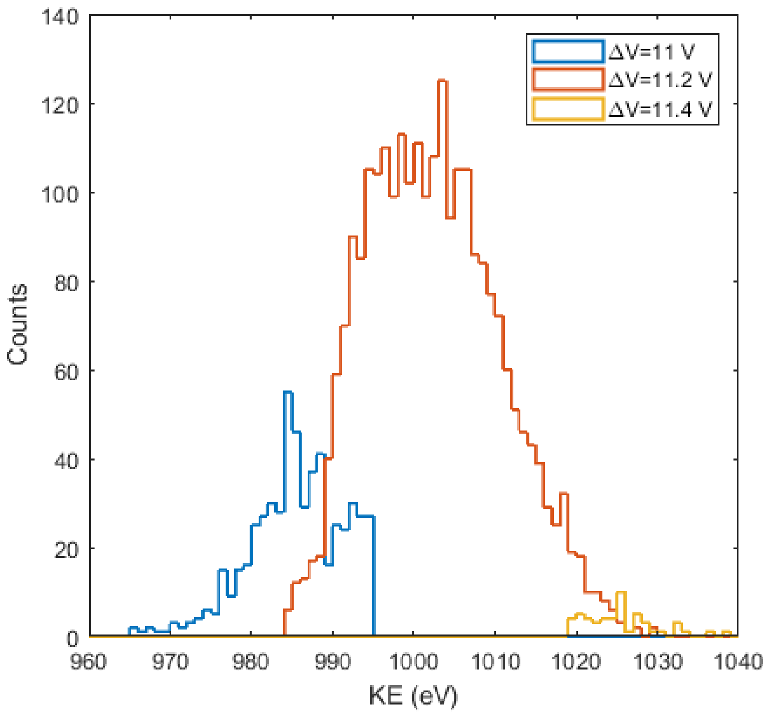

Figure 18: Energy distribution of Sn-120 ions with charge states ranging from 3 to 5 using an aperture of 1.0 mm for different voltage differences ΔV.

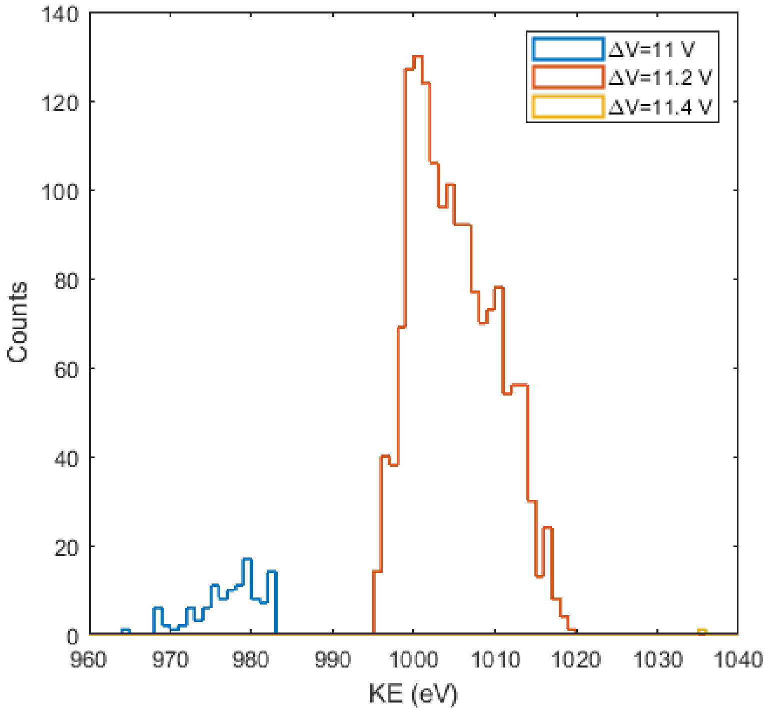

Figure 19: Energy distribution of Sn-120 ions with charge states ranging from 3 to 5 using an aperture of 0.5 mm for different voltage differences ΔV.

It follows from the graphs that for a smaller aperture, less particles come through. However, the energy range decreases as well, which leads to more accurate measurements. The aperture of 0.5 mm shows a shift from the expected 1 keV, this is probably due to the slightly higher $\Delta V = 11.2\ V$ compared to the optimal $\Delta V = 11.14\ V$. It also shows that for $\Delta V < \Delta V_{optimal}$, the Wien Filter acts as a low-pass filter and for $\Delta V > \Delta V_{optimal}$ acts as a high-pass filter.

5.2.3 Tubes

Figure 8 shows the disassembled Wien Filter. The tubes are not perfectly parallel to the electrodes but show a slight angle. To investigate the effect of this misalignment on the measured energy distribution, a model is used where the right tube is located at an angle of about 0.4°. A simulation is done for the aperture of 0.5 mm and with the same 3000 particle Sn-120 beam as used for the different apertures. The results are shown in figure 20.

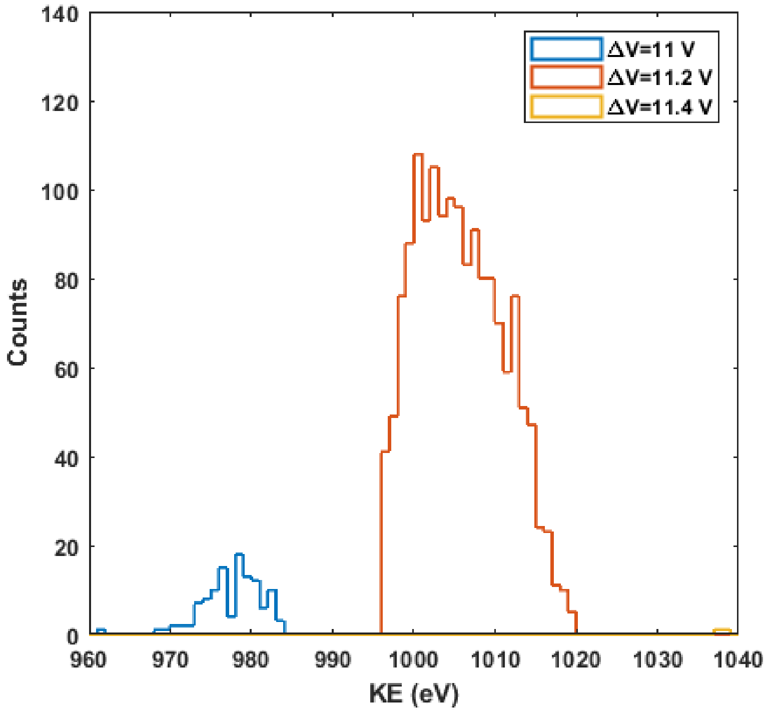

Figure 20: Energy distribution of Sn-120 ions with charge states ranging from 3 to 5 using an aperture of 0.5 mm for different voltage differences ΔV and an angle of 0.4° for the right tube.

Comparing figures 20 and 19, it shows that the energy ranges are similar. But figure 19 shows a higher count for particles near 1002 eV. The total counts for $\Delta V = 11.2\ V$ for the parallel and tilted tube are $N_p = 1573$ and $N_t = 1558$ respectively.

5.2.4 Electrodes

During reassembly of the Wien Filter it is not guaranteed that both electrodes will be aligned perfectly parallel. A SIMION model is created with a shift in the negative x-direction of 50 μm in the second half of the upper electrode, creating an almost parallel alignment. The same input beam as the tube and aperture simulations is used. The results are shown in figure 21.

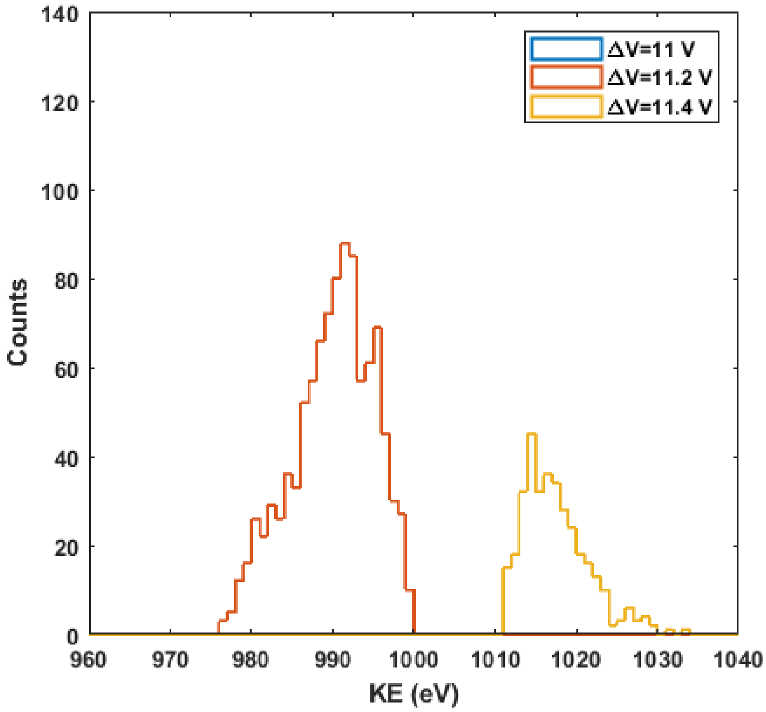

Figure 21: Energy distribution of Sn-120 ions with charge states ranging from 3 to 5 using an aperture of 0.5 mm for different voltage differences ΔV for misaligned electrodes.

Figure 21 shows a completely shifted distribution compared to the parallel aligned electrode measurement, figure 19. The total counts for $\Delta V = 11.2\ V$ is $N_e = 1007$, which is significantly lower than the aligned setup with $N_p = 1573$.

6 Discussion

The Time of Flight simulation shows a normal distribution for the time delay. However this is for ideal circumstances where all the particles travel in the same direction without any scattering angle. To determine the energy distribution using the Time of Flight method, the beam may have to be focused in order not to miss too many particles.

The simulations of the different magnetic yokes of the Wien Filter showed that it can not be used to uniquely identify all different charge states with the same 1 keV energy distribution. This is due to the fact that the Wien condition is satisfied for a certain kinetic energy of a particle. To determine the different charge states, the energy distribution of each charge state has to be slightly different from each other. If so, the high- and low-pass filter option of the Wien Filter might be of benefit.

Which aperture to use is a trade off between better transmission and better resolution. It is suggested to first run measurements with the larger apertures to get a rough range for the voltage difference

ΔV. Then the smaller aperture can be used for more accurate measurements, as it shows an energy range of around 25 eV.

The effect of the slightly tilted tube is negligible. The tubes are present to reduce the stray electric and magnetic fields. Therefore if the ion beam does not collide with the beginning of the tube, there should not be a noticeable impact on the measurements. However the alignment of the electrodes is very crucial, even a small shift of the electrodes resulted in a shift of the energy distribution on the order of 15 eV.

The theory of the Wien Filter works with some assumptions. The first one is a perfect electric and magnetic field. However in real measurements this is not the case. The tubes are placed to approach the assumption, but do not block all the effect of the fields. For the simulation the electric field was simulated by two electrodes, which gives an electric field with a stray field on both sides of the electrodes. The magnetic field was simulated with a user program and placed directly on the electrodes. Therefore no stray magnetic field is present in the simulations, which could have affected the measurements. The other assumption is that the Sn-120 ions travel in the z-direction, without any angle and all from the same origin. In reality this is not the case, as they have a certain scatter angle due to the collisions with the hydrogen gas. Therefore the ion beam after collisions may have to be focused just as with the Time of Flight.

For further research another SIMION model should be made with the magnetic field simulated such that it does have a stray field to see if it noticeably affects the measurements. SIMION gives an option to give a distribution to the starting angle at which the particles travel and a distribution in the starting position. Additional simulations should be done to determine the effects of these starting parameters. Also further research should be done using the real Wien Filter to compare those results with the results of the simulation.

7 Conclusion

For the Time of Flight simulation, the FWHM of the time delay is calculated to be a factor 3 or 4 higher than the FWHM of the bunch length. Which makes the effect of the bunch length on the Time of Flight method negligible. Therefore the Time of Flight method could prove useful to determine the energy of the energetic tin ions after traversing the stopping gas.

The Wien Filter simulations show that both the strong and weak magnetic yoke are unable to fully differentiate the different charge states of the tin ions if each charge state has the same energy distribution. Simulations using the strong magnetic yoke showed that the high-pass nature of the Wien Filter could help to get information on the fraction of ions that loose an appreciable part of their kinetic energy (10–20 eV). The simulations using the weak magnetic yoke showed that for $\Delta V < \Delta V_{optimal}$, the Wien Filter acts as a low-pass filter and for $\Delta V > \Delta V_{optimal}$ acts as a high-pass filter. If different charge states have different energy distributions, the Wien Filter can be used to distinguish different charge states.

8 Acknowledgements

Even though my bachelor project did not go as I expected due to the pandemic, I am still grateful for the time and experience of being part of the QISD group. Firstly I want to thank Ronnie Hoekstra for the opportunity to take part in his research group and for finding an alternative solution to the experimental research. Secondly I want to thank Subam Rai for the sessions to help me with SIMION and for the feedback on my results. I would like to thank Mart Salverda for his work on disassembling the Wien Filter to provide me with the necessary dimensions and drawings for my reseach. I would also like to thank Klaas Bijlsma for his input and knowledge during the meetings and for providing me with the Wien Filter manual and data I needed. Lastly, I would like to thank all the members of the QISD group for the interesting and informative Zoom meetings I had.

References

[1] "Over 50 years of moore's law." [Online], Available at: https://www.intel.com/content/www/us/en/silicon-innovations/moores-law-technology.html (Accessed: July 2020).

[2] Tardi, C (2019) Moore's law, Available at: https://www.investopedia.com/terms/m/mooreslaw.asp (Accessed: July 2020).

[3] "Big steps in tiny patterns." [Online], Available at: https://www.asml.com/en/technology (Accessed: July 2020).

[4] Wang, B (2017) EUV Lithography tools shipping in 2018, Available at: https://www.nextbigfuture.com/2017/04/euv-lithography-tools-shipping-in-2018.html (Accessed: July 2020).

[5] M Barat and P Roncin 1992 J. Phys. B: At. Mol. Opt. Phys. 25 2205

[6] Brinkhuis, E. S. (2020). Energetic ions traversing hydrogen gas: charge exchange reactions and pulse length considerations. [Groningen]: Rijksuniversiteit Groningen.

[7] Deuzeman, M. J. (2019). Generation and interactions of energetic tin ions. [Groningen]: Rijksuniversiteit Groningen.

[8] DREEBIT (2015). Instruction Manual: Wien Filter (version 1.0)

[9] Lubinski, G. (2001). Light - a fingerprint of astrophysical processes. Groningen: s.n.

[10] Manura, D. (2008). SIMION® 8.0 User Manual. Scientific Instrument Services. https://SIMION.com/manual/chap2.html